Confocal reflectance microscopy for determination of microbubble resonator thickness

Alessandro Cosci,[1,2,*] Franco Quercioli,[3] Daniele Farnesi,[1,2] Simone Berneschi,[2] Ambra Giannetti,[2] Franco Cosi,[2] Andrea Barucci,[2] Gualtiero Nunzi Conti,[1,2] Giancarlo Righini [1,2] and Stefano Pelli [1,2]

[1]*Museo Storico della Fisica e Centro Studi e Ricerche Enrico Fermi, Piazza del Viminale 1, 00184 Rome, Italy*
[2]*IFAC-CNR, Istituto di Fisica Applicata "Nello Carrara", Consiglio Nazionale delle Ricerche, Via Madonna del Piano 10, 50019 Sesto Fiorentino, Italy*
[3]*INO-CNR, Istituto Nazionale di Ottica Consiglio Nazionale delle Ricerche, Largo Enrico Fermi 6, 50125 Arcetri-Firenze, Italy*
[*]*a.cosci@ifac.cnr.it*

Abstract: Optical Micro Bubble Resonators (OMBR) are emerging as new type of sensors characterized by high Q-factor and embedded micro-fluidic. Sensitivity is related to cavity field penetration and, therefore, to the resonator thickness. At the state of the art, methods for OMBR's wall thickness evaluation rely only on a theoretical approach. The purpose of this study is to create a non-destructive method for measuring the shell thickness of a microbubble using reflectance confocal microscopy. The method was validated through measurements on etched capillaries with different thickness and finally it was applied on microbubble resonators.

OCIS codes: (140.3948) Microcavity devices; (140.4780) Optical resonators; (280.4788) Optical sensing and sensors.

References and links

1. S. Berneschi, D. Farnesi, F. Cosi, G. N. Conti, S. Pelli, G. C. Righini, and S. Soria, "High *Q* silica microbubble resonators fabricated by arc discharge," Opt. Lett. **36**(17), 3521–3523 (2011).
2. X. Zhang, L. Liu, and L. Xu, "Ultralow sensing limit in optofluidic micro-bottle resonator biosensor by selfreferenced differential-mode detection scheme," Appl. Phys. Lett. **104**(3), 033703 (2014).
3. J. Ward, Y. Yang, R. Madugani, and S. N. Chormaic, "Sensing and optomechanics using whispering gallery microbubble resonators," in *Photonics Conference (IPC)*, (IEEE, 2013), pp. 452–453.
4. R. Henze, T. Seifert, J. Ward, and O. Benson, "Tuning whispering gallery modes using internal aerostatic pressure," Opt. Lett. **36**(23), 4536–4538 (2011).
5. W. Lee, Y. Sun, H. Li, K. Reddy, M. Sumetsky, and X. Fan, "A quasi-droplet optofluidic ring resonator laser using a micro-bubble," Appl. Phys. Lett. **99**(9), 091102 (2011).
6. M. Li, X. Wu, L. Liu, and L. Xu, "Kerr parametric oscillations and frequency comb generation from dispersion compensated silica micro-bubble resonators," Opt. Express **21**(14), 16908–16913 (2013).
7. D. Farnesi, A. Barucci, G. C. Righini, S. Berneschi, S. Soria, and G. Nunzi Conti, "Optical Frequency Conversion in Silica-Whispering-Gallery-Mode Microspherical Resonators," Phys. Rev. Lett. **112**(9), 093901 (2014).
8. M. Sumetsky, Y. Dulashko, and R. S. Windeler, "Optical microbubble resonator," Opt. Lett. **35**(7), 898–900 (2010).
9. Y. Yang, J. Ward, and S. N. Chormaic, "Quasi-droplet microbubbles for high resolution sensing applications," Opt. Express **22**(6), 6881–6898 (2014).
10. H. Li, Y. Guo, Y. Sun, K. Reddy, and X. Fan, "Analysis of single nanoparticle detection by using 3-dimensionally confined optofluidic ring resonators," Opt. Express **18**(24), 25081–25088 (2010).
11. T. Wilson and C. Sheppard, *Theory and Practice of Scanning Optical Microscopy* (Academic, 1984).
12. G. Cox and C. J. R. Sheppard, "Measurement of thin coatings in the confocal microscope," Micron **32**(7), 701–705 (2001).
13. C. J. R. Sheppard, T. J. Connolly, J. Lee, and C. J. Cogswell, "Confocal imaging of a stratified medium," Appl. Opt. **33**(4), 631–640 (1994).
14. M. Born and E. Wolf, *Principle of Optics* (Cambridge,1999).

#240121 Received 30 Apr 2015; revised 4 Jun 2015; accepted 5 Jun 2015; published 16 Jun 2015

15. J. F. Aguilar, M. Lera, and C. J. R. Sheppard, "Imaging of spheres and surface profiling by confocal microscopy," Appl. Opt. **39**(25), 4621–4628 (2000).
16. H. Jacobsen and S. Hell, "Effect of the specimen refractive index on the imaging of a confocal fluorescence microscope employing high aperture oil immersion lenses," Bioimaging **3**(1), 39–47 (1995).
17. T. H. Besseling, J. Jose, and A. Van Blaaderen, "Methods to calibrate and scale axial distances in confocal microscopy as a function of refractive index," J. Microsc. **257**(2), 142–150 (2015).
18. W. Weise, P. Zinin, T. Wilson, A. Briggs, and S. Boseck, "Imaging of spheres with the confocal scanning optical microscope," Opt. Lett. **21**(22), 1800–1802 (1996).
19. C. J. R. Sheppard and H. J. Matthews, "Imaging in high-aperture optical systems," J. Opt. Soc. Am. A **4**(8), 1354 (1987).
20. G. R. Brady and J. R. Fienup, "Nonlinear optimization algorithm for retrieving the full complex pupil function," Opt. Express **14**(2), 474–486 (2006).
21. J. E. N. Jonkman and E. H. K. Stelzer, "Resolution and contrast in confocal and two-photon microscopy," in *Confocal and Two-photon Microscopy: Foundations, Applications, and Advances*, A. Diaspro Ed., Wiley-Liss, Inc., New York (2002).
22. X. Fan, I. M. White, S. I. Shopova, H. Zhu, J. D. Suter, and Y. Sun, "Sensitive optical biosensors for unlabeled targets: A review," Anal. Chim. Acta **620**(1-2), 8–26 (2008).

1. Introduction

Optical Micro Bubble Resonators (OMBR) are a new promising tool for optical sensing, due to their high Q-Factor and embedded micro-fluidics [1]. Indeed, OMBRs have been already studied for biomarker [2], temperature [3] and pressure [4] sensing. Furthermore, OMBRs are suitable for studying ring resonator lasers [5] and non-linear effects as Kerr effect [6] and third-harmonic-generation [7]. At the state of the art, OMBR production relies on two main methods: high voltage arc discharge [1] or CO_2 laser [8] capillary heating, both coupled to inflating the capillary at controlled pressure. Sensing capability is related to the intensity of the electromagnetic field inside the hollow cavity, and field distribution is strongly dependent on OBMR thickness [9, 10]. Therefore, it is extremely important to evaluate this parameter to assess OMBR capabilities and sensitivity. Previous studies used either theoretical [4, 8] or destructive [5] methods to evaluate OMBR thickness. However, a noninvasive and non-destructing method for measuring the thickness could be useful to monitor in-line OMBR production. Confocal reflectance imaging is a standard technique for measuring and imaging changes in refractive index [11]. Previous works already demonstrated its capability for measuring thin film thickness [12, 13] and for imaging the profile of metallic spheres [14, 15]. In the neighborhood of the imaging pole, an OMBR may be assumed as a thin slab of fused silica in air. Therefore, it is possible to use confocal reflectance imaging for OMBR thickness measurement. Resonators were imaged at different focal depths (z-scan). For each medium interface corresponds an intensity peak. By calculating the distance between the two material interface peaks it is possible to measure an apparent value of the OMBR wall-thickness. The real value for thickness can be obtained, starting from the apparent value and considering the refractive index of the media and the angular spectrum of the objective. This study followed the approach presented in [12], where thin film thicknesses were retrieved by means of a calibration curve. The method was validated using thin etched capillaries with [resulting] different thicknesses. The values obtained using the z-scan images and the reflection peaks were compared with those calculated by imaging the orthogonal section of the cut capillaries. Then, a simple theoretical model for OMBR thickness determination, based on a geometrical approach considering the capillary expansion, was used to estimate the possible range of thickness values. Finally, we measured the OMBR thickness by confocal reflectance imaging: the obtained values are in agreement with our theoretical model.

2. Materials and methods

2.1 Fused silica capillaries

Fused silica capillaries with two different inner (ID) and outer (OD) diameter were used (ID 100 μm, OD 140 μm and ID 200 μm, OD 240 μm), both having a wall thickness of 20 μm

#240121 Received 30 Apr 2015; revised 4 Jun 2015; accepted 5 Jun 2015; published 16 Jun 2015

(Z-FSS-100165 and Z-FSS-200280, Postnova, Germany). In order to calibrate the method, five different wall thicknesses were created starting from the capillary with ID = 200 μm. Calibration samples were made by chemically etching the outer surface of the capillaries by using 40% hydrofluoric acid (HF). Etching time varied from 240 to 960 seconds.

2.2 Microbubble production

Microbubble resonators were produced by applying a high voltage arc discharge in the proximity of a pressurized capillary as described in [1]. The high temperature obtained by arc discharge quickly melts a localized section of the capillary. By applying a pressure of 1.2 Bar, insuffling pure Argon, melted silica expands isotropically and creates a microbubble resonator along the capillary. Final outer diameters of microbubble are ranging from 256 μm to 480 μm and from 439 μm to 665 μm for capillaries with starting ID of 100 μm and 200 μm, respectively.

2.3 Theoretical approach

Microbubble shell thickness can be calculated theoretically using a geometrical approach. During the melting and expansion stages, it is possible to make two different assumptions based on mass conservation. In the first assumption, it is considered that the area of the shell of the capillary is conserved. The final OMBR can be thought as the result of a cylindrical expansion of the silica capillary. If an orthogonal section of the capillary, prior the expansion, is considered, a ring with the following area will be obtained:

$$a = \pi r^2 - \pi(r-\delta)^2 \approx 2\pi r\delta \tag{1}$$

where r is the outer radius and δ is the thickness. Since $\delta << r$ (about 1/10) the δ^2 term, compared to the term $r\delta$, in a first approximation can be neglected. If we then consider the microbubble at the equator, the area of the expanded ring is

$$A = \pi R^2 - \pi(R-\Delta)^2 \approx 2\pi R\Delta \tag{2}$$

where R is the outer radius and Δ is the thickness. If it is assumed that, during the expansion, the area is preserved, i.e. $a = A$, the following relation is then obtained:

$$\frac{\Delta}{\delta} = \frac{r}{R} \tag{3}$$

This result is a simplification of the formula proposed in [4].

In the second assumption, the volume is preserved. The OMBR can be thought as a spherical expansion of an initial bubble with the same radius of the capillary. Therefore, considering a starting spherical shell with radius r and a thickness δ, and a final shell of thickness Δ and radius R and assuming the two shell volumes to be equal, i.e. $v = V$, it is obtained:

$$\frac{\Delta}{\delta} = \frac{r^2}{R^2} \tag{4}$$

It has to be noticed that in the first case the thickness decreases linearly with the bubble radius, while in the second one the decrease is quadratic. It is reasonable to assume that the cylindrical expansion is an over-estimation of the capillary thickness, therefore the upper limit for the measured thickness. Vice versa, the lower limit is represented by the spherical approximation.

2.4 Reflectance confocal microscope

The microscope used was a BioRad 1024 ES with 488 nm excitation wavelength and a 40X, 0.75 NA air objective. The choice of the objective relies on the high reflection contrast of

#240121 Received 30 Apr 2015; revised 4 Jun 2015; accepted 5 Jun 2015; published 16 Jun 2015

air/silica interface and a NA high enough for a good resolution but not too high in order to reduce scattering and aberration effects. Microbubble resonators and capillaries were imaged at different depths by a z-scan, using steps of 0.2 µm. Every image is a square area of 270 µm x 270 µm divided in a grid of 512 px times 512 px.

2.5 Confocal thickness measurements

When using a confocal microscope for thickness measurements one has to take into account that, due to refractive index mismatch, the measured objective displacement does not correspond to the effective focal point displacement inside the sample [16, 17]. This work uses the approach described in [12, 13, 18], simulating the output signal from a thin silica slab, at different focal depths, imaged by a reflectance confocal microscope. As a result, a *z* profile with two strong peaks, corresponding to the two medium interfaces, was obtained. A simulated retrieved signal by a reflectance confocal microscope of a fused silica slab in air is presented in Fig. 1(a). At every peak distance corresponds a slab thickness. A Matlab (Matlab, The Mathworks Inc., MA, USA) routine was used to simulate *z* profiles arising from slabs of variable thickness from 2 µm to 20 µm, using a 0.1 µm step, as described in [12, 13, 16]. A calibration curve was obtained, Fig. 1(b).

Both OMBR and capillaries were imaged at different depths using the confocal reflectance microscope. By selecting a point in the first image of the z-stack, it is possible to retrieve a z profile. By calculating the peaks distance and finding back this value in the calibration curve it is possible to calculate the real thickness of the sample corresponding to the selected point.

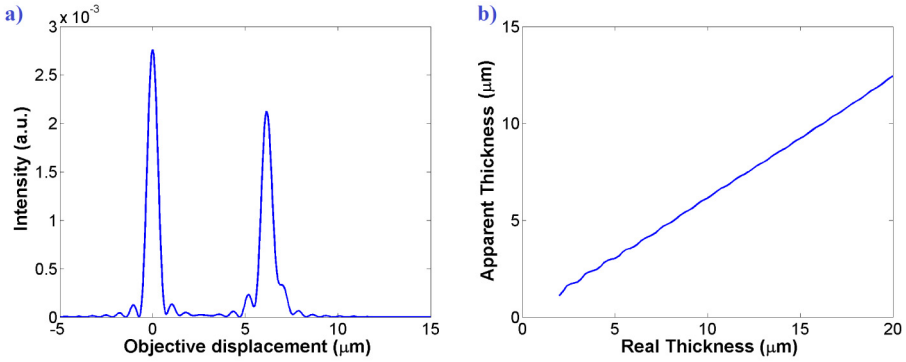

Fig. 1. Simulated output signal by a confocal microscope from a thin fused silica slab of 10 µm in air (a). Calibration curve obtained by the peaks distance from the simulated signal from fused silica slabs in air with varying thicknesses from 2 µm to 20 µm.

In the case of OMBR the interface is spherical and not planar. Anyway, using the transfer matrix for a spherical interface, instead of the one for a planar interface, the only term affected is the derivative one:

$$\frac{dx_2}{dz} = \frac{n_1 - n_2}{n_2}\frac{x_1}{R} + \frac{n_1}{n_2}\frac{dx_2}{dz} \tag{5}$$

where z is the optical axis, n_1 and n_2 are the refractive indexes of air and fused silica, respectively, x_1 and x_2 are the distance from the optical axis before and after the interface and R is the sphere radius. The second term corresponds to the bare slab configuration. Using a 0.75 NA objective, for focal depth values in the order of 10 µm, the first term is well below 2%, therefore the OMBR interface can be thought as a thin slab.

#240121 Received 30 Apr 2015; revised 4 Jun 2015; accepted 5 Jun 2015; published 16 Jun 2015

For the validation through the etched capillaries, wall-thickness was considered the average of the values retrieved from five points along the central symmetry axis. Uncertainty was assessed as the system scanning resolution (0.6 μm).

For each OMBR, an area of 10.54 μm x 10.54 μm (20 px x 20px), centered at the resonator transversal pole, was selected. For each *xy*-pixel of the area, a *z*-axis intensity profile was retrieved and the corresponding resonator wall-thickness was calculated. The average of the obtained values was chosen as the effective resonator wall thickness.

2.6 Orthogonal thickness measurements

Effective thickness of etched capillaries was measured by means of confocal imaging of an orthogonal section obtained by using a fiber-cutter. For each capillary, we performed a z-scan, under the same condition described above, through the orthogonal section. Images obtained had a typical ring-shape and were processed by a Matlab routine. The reflectance intensity profile along the radius of the capillary tip was retrieved. Thickness value was calculated by measuring the spatial difference between the two highest derivative values of the fluorescence profile.

3. Results and discussion

3.1 Measurements on etched capillaries towards confocal technique validation

A typical z-stack image, with its orthogonal views, of an etched capillary is shown in Fig. 2. It is possible to note that, as expected, the *zy* section represents a slab, Fig. 1b, while the *xz* profile is a circular shell, Fig. 2(c) Fig. 2(d) shows the intensity *z*-profile retrieved from a central point belonging to the symmetry axis of the capillary. By using the calibration curve, it was possible to evaluate the capillary thickness.

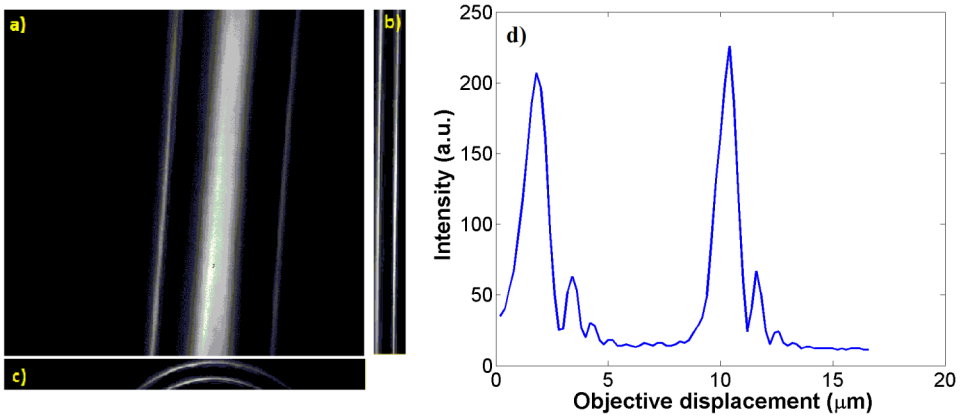

Fig. 2. Planar section of the z-stack correspondent to the interface of fused silica with air inside the hollow capillary core (a) and orthogonal views along the two axis (b,c). Intensity profile taken along the symmetry axis is shown in (d).

In order to obtain direct measurements, capillaries were orthogonal cut and imaged. An example image from the orthogonal view of the capillary is represented in Fig. 3(a), while in Fig. 3(b) the correspondent intensity profile taken along the wall thickness (yellow line in Fig. 3(a)) is shown.

#240121 Received 30 Apr 2015; revised 4 Jun 2015; accepted 5 Jun 2015; published 16 Jun 2015

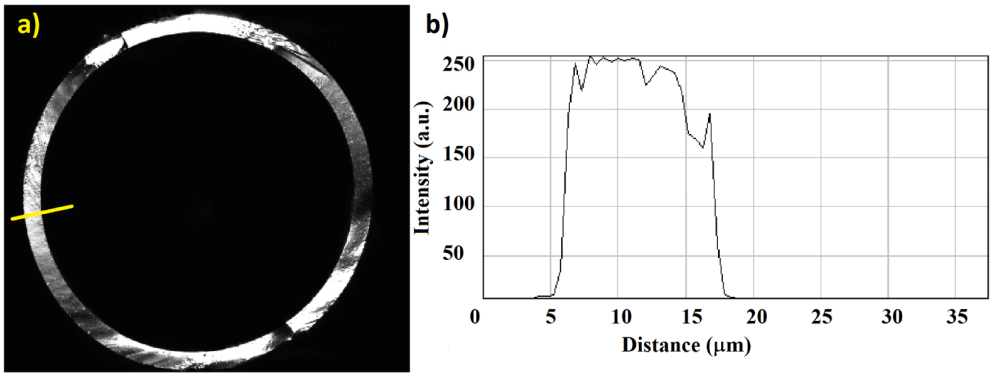

Fig. 3. Confocal microscope image of a section of fused silica capillary (a) and correspondent intensity profile taken along the yellow line (b).

The capillary orthogonal section shows its typical ring-shape, from which it was possible to directly measure the thickness. Both direct and confocal measurements are plotted versus etching time in Fig. 4.

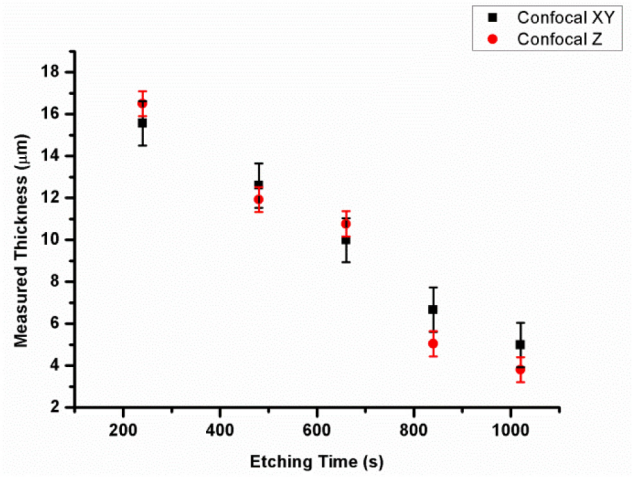

Fig. 4. Capillary thickness versus etching time measured through confocal reflectance microscopy along the Z axis (red) and orthogonal XY cut (black).

Since thickness measurement arises from a distance difference between the peaks, uncertainty in the Z confocal measurements was considered as the double of the accuracy in the objective displacement, also taking into account the calibration curve (0.6 μm). For the orthogonal XY measurements uncertainty was evaluated as twice the system scanning resolution (2 x 0.527 μm).

The two different measurements are in good agreement, validating the use of Z confocal reflectance microscopy for thickness evaluation of the microbubble.

3.2 Measurements on microbubble resonators

After the validation of the technique for thickness evaluation, twenty microbubble resonators were investigated under the microscope (8 with starting capillary OD of 140 μm and 12 with starting capillary OD of 240 μm). Microbubbles differ for original ID of the capillary and for final outer bubble diameter. For each resonator a full 3D z-stack image was obtained. As it can be seen in Fig. 5, resonators can show a circular, Fig. 5(a), or double ring shape, Fig. 5(b), depending on focal depth. Both orthogonal views show circular shells as expected.

#240121 Received 30 Apr 2015; revised 4 Jun 2015; accepted 5 Jun 2015; published 16 Jun 2015

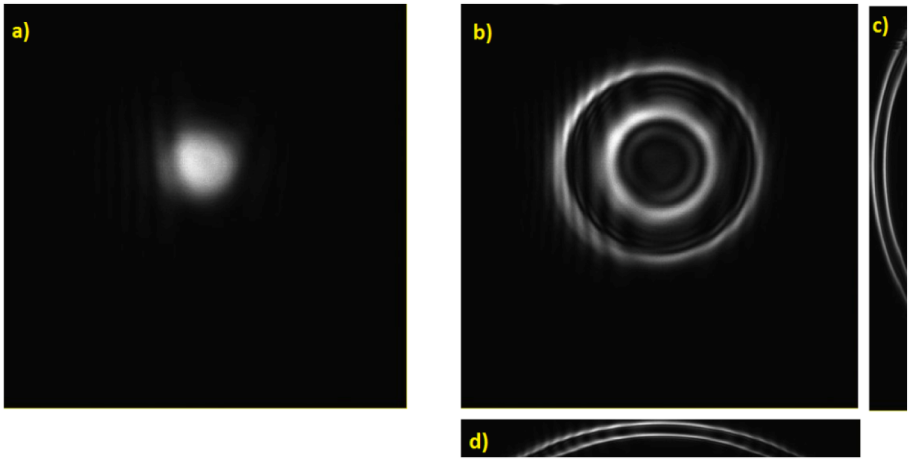

Fig. 5. Z-stack images corresponding to the first air to silica interface at the outer shell of the bubble resonator (a) and at 10 µm depth (b). Orthogonal views along the two different axis are represented in (c), (d).

As it can be noticed in Fig. 5, obtained images are distorted by interference patterns mainly due to scattering effects from the resonator [15, 16] and objective aberrations [19, 20]. Nevertheless, interference peaks do not seem to influence the thickness measurements.

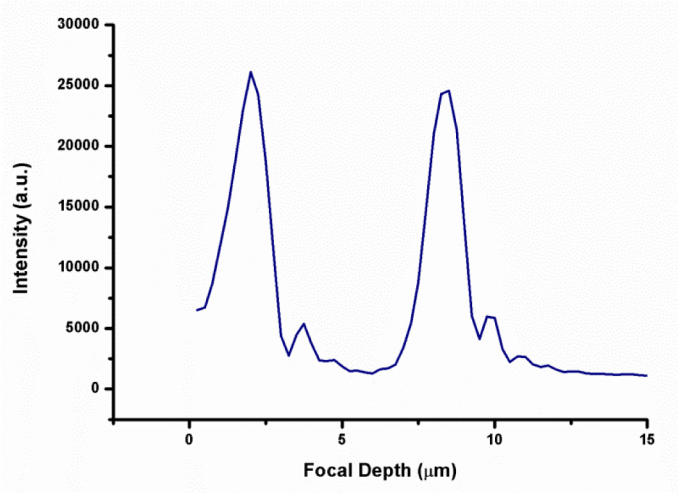

Fig. 6. Intensity profile along the z-axis at the resonator center.

An intensity profile taken from the center of the resonator image along the xy-plane is represented in Fig. 6. The two reflection peaks are clearly observable. Then, by using the calibration curve, it was possible to retrieve the effective resonator thickness in the selected point. Final OMBR wall-thickness was evaluated as the average of the calculated values on an area of 10.54 µm x 10.54 µm (20 px x 20px), centered at the resonator transversal pole. Figure 7(a) shows the measured wall thicknesses for OMBRs obtained from capillaries with OD of 140 µm. Figure 7(b) shows the measured wall thicknesses for OMBRs with capillary's OD of 240 µm.

#240121 Received 30 Apr 2015; revised 4 Jun 2015; accepted 5 Jun 2015; published 16 Jun 2015

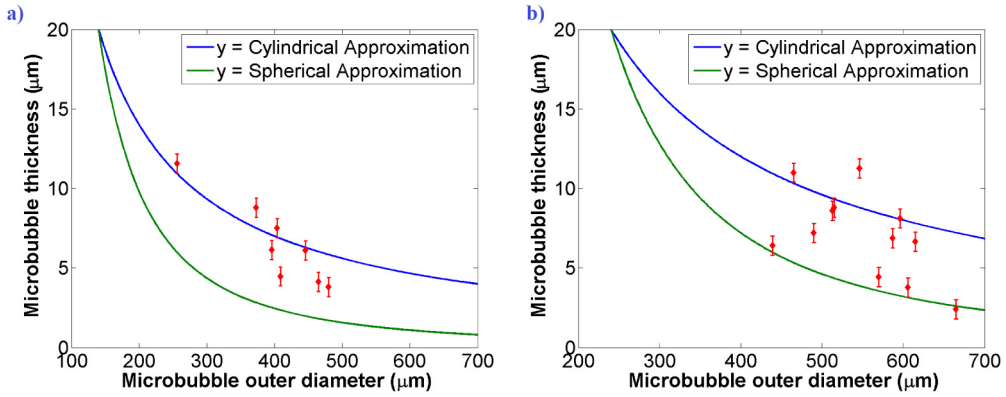

Fig. 7. Measured microbubble thickness versus resonator radius. OMBRs were produced from two different capillaries having OD of 140 μm (a) and 240 μm (b). The two lines represent two different approximations. As described above, the cylindrical approximation (blue) gives the upper theoretical limit for the OMBR thickness, whilst the spherical approximation (green) represents the lower limit.

As expected, most of the measured thicknesses are lying between the two theoretical limits. Anyway, few points were found above the cylindrical limit. There could be several explanations for this fact. It was observed that the capillaries were getting shorter while exposed to the arc discharge during resonator fabrication. Hence, microbubbles may have drawn fused silica from nearby areas. Furthermore, we must point out that in a first phase the inner pressure is perpendicular to the capillary parallel surface, promoting cylindrical expansion. During the expansion, the surface starts to get more circular, favoring spherical expansion. Therefore, it could be expected that, for small final outer diameters of the resonator, the thickness should be closer to the cylindrical approximation, whilst it will move toward the spherical limit as the resonator is getting larger. Furthermore, outliers values can arise from OMBR asymmetries, which were not taken into account in this work. As described above, OMBRs are presently produced by two parallel arc discharges, which may not guarantee perfect symmetry. However, the final OD was always checked along both axes, parallel and orthogonal to the sparks. Possible asymmetries were found to be lower than 5%. Finally, this work did not take into account all the parameters used for OMBR production as pressure and arc discharge time duration. Different parameters can promote different expansion and, hence, affect whether the expansion obeys more to cylindrical or spherical approximation.

Even though confocal reflectance microscopy has found to be suitable for OMBR wall-thickness evaluation, it must be pointed out that this method is limited by the confocal axial resolution of the microscope. Considering the refractive index of air and fused silica, and taking into account a working wavelength of 488 nm and an objective with NA of 0.75, it is possible to obtain a microscope resolution of 1.78 μm [21]. Below this value, as in the case of quasi-droplets resonators, it would not be possible to retrieve valid values for the OMBR wall-thickness. However, this limit can be reduced by using a shorter wavelength laser source and increasing the NA of the objective. In fact, this method revealed to be useful for non-destructive monitoring of OMBR production and, furthermore, it allows to assess an important parameter for sensing applications. It is also worth pointing out that wall thicknesses of a few micrometers (rather than sub-micrometer as in the case of quasi-droplet) are mainly used for critical applications like for instance label-free biosensing [22].

4. Conclusion

In this manuscript it was demonstrated that confocal reflectance is a non-invasive and non-destructive effective method for OMBR thickness measurement. It was shown that, for radius

#240121 Received 30 Apr 2015; revised 4 Jun 2015; accepted 5 Jun 2015; published 16 Jun 2015

of curvature and for thickness of the order of 250 μm and 10 μm, respectively, it is possible to use the method proposed by Sheppard et al. [12] for thin films. The method was first tested on etched capillaries with different thicknesses. Measurements obtained by the calibration curve are in good agreement with the ones made using the conventional imaging of orthogonally cut capillaries. A simple theoretical model for thickness range value calculation was proposed. Finally, twenty different OMBRs with different original and final outer diameter were measured. Most of the evaluated wall-thicknesses fit in the two theoretical limits. This method can be then used for monitoring the OMBR fabrication process in order to guarantee reproducibility and obtain sensing devices with optimized characteristics.

Acknowledgments

The authors wish to acknowledge the financial support of the Ministero dell'Istruzione, dell'Università e della Ricerca (MIUR) through the Centro Fermi project "Premiale 2012 - Fisica e strumentazione per la salute dell'uomo" and Futuro in Ricerca (FIR) programme - grant N. RBFR122KL1 (SENS4BIO). S. Berneschi wishes to thank MIUR for its support through PRIN 2010-2011 Project ARTEMIDE (ref. 20108ZSRTR).

#240121 Received 30 Apr 2015; revised 4 Jun 2015; accepted 5 Jun 2015; published 16 Jun 2015